



**HAL**  
open science

## Cesium gas strongly confined in one dimension : sideband cooling and collisional properties

Isabelle Bouchoule, M. Morigana, Christophe Salomon, D. Petrov

### ► To cite this version:

Isabelle Bouchoule, M. Morigana, Christophe Salomon, D. Petrov. Cesium gas strongly confined in one dimension : sideband cooling and collisional properties. *Physical Review A : Atomic, molecular, and optical physics [1990-2015]*, 2002, 65, pp.033402. 10.1103/PhysRevA.65.033402 . hal-00001587

**HAL Id: hal-00001587**

**<https://hal.science/hal-00001587>**

Submitted on 14 Apr 2016

**HAL** is a multi-disciplinary open access archive for the deposit and dissemination of scientific research documents, whether they are published or not. The documents may come from teaching and research institutions in France or abroad, or from public or private research centers.

L'archive ouverte pluridisciplinaire **HAL**, est destinée au dépôt et à la diffusion de documents scientifiques de niveau recherche, publiés ou non, émanant des établissements d'enseignement et de recherche français ou étrangers, des laboratoires publics ou privés.

# Cesium gas strongly confined in one dimension: Sideband cooling and collisional properties

I. Bouchoule, M. Morinaga,\* and C. Salomon

*Laboratoire Kastler Brossel, 24 rue Lhomond, 75231 Paris, France*

D. S. Petrov

*FOM Institute for Atomic and Molecular Physics, Kruislaan 407, 1098 SJ Amsterdam, The Netherlands  
and Russian Research Center, Kurchatov Institute, Kurchatov Square, 123182 Moscow, Russia*

(Received 6 June 2001; published 1 February 2002)

We study one-dimensional (1D) sideband cooling of cesium atoms strongly confined in a far-detuned optical lattice. The Lamb-Dicke regime is achieved in the lattice direction whereas the transverse confinement is much weaker. The employed sideband cooling method, first studied by Vuletić *et al.*, uses Raman transitions between Zeeman levels and produces a spin-polarized sample. We present a detailed study of this cooling method and investigate the role of elastic collisions in the system. We accumulate 83(5)% of the atoms in the vibrational ground state of the strongly confined motion, and elastic collisions cool the transverse motion to a temperature of  $2.8 \mu\text{K} = 0.7\hbar\omega_{\text{osc}}/k_B$ , where  $\omega_{\text{osc}}$  is the oscillation frequency in the strongly confined direction. The sample then approaches the regime of a quasi-2D cold gas. We analyze the limits of this cooling method and propose a dynamical change of the trapping potential as a mean of cooling the atomic sample to still lower temperatures. Measurements of the rate of thermalization between the weakly and strongly confined degrees of freedom are compatible with the zero-energy scattering resonance observed previously in weak 3D traps. For the explored temperature range the measurements agree with recent calculations of quasi-2D collisions. Transparent analytical models reproduce the expected behavior for  $k_B T \gg \hbar\omega_{\text{osc}}$  and also for  $k_B T \ll \hbar\omega_{\text{osc}}$  where the 2D features are prominent.

DOI: 10.1103/PhysRevA.65.033402

PACS number(s): 32.80.Pj, 34.50.-s

## I. INTRODUCTION

The physics of systems with reduced spatial dimensionality has attracted a great deal of interest. These systems, where one (two) degree(s) of freedom are confined to the quantum ground state of motion, have properties that can markedly differ from those of three-dimensional (3D) systems. The case of a 2D Bose gas has been explored theoretically and experimentally with atomic hydrogen adsorbed on liquid helium (see [1,2]). Advances on laser cooling and Bose-Einstein condensation of atomic gases [3] have opened an interesting possibility to create new 1D and 2D quantum degenerate systems [4,5]. In a recent paper Petrov, Holzmann, and Shlyapnikov showed that collisional properties of cold gases can be drastically modified by strongly confining the motion of particles in one direction [4]: for instance, in a gas with negative scattering length  $a$ , the mean-field interaction can switch sign under variations of the strong confinement. This is of particular interest for the case of cesium. Due to a very large and negative scattering length  $a = -138 \text{ nm}$  in the  $|F=3, m=3\rangle$  state [6], a cesium condensate in a weakly confining trap would be unstable for a few tens of atoms [7]. The characteristic size of the quantum ground state in the strongly confined direction is another important length in this problem. For a harmonic potential with oscillation frequency  $\omega_{\text{osc}}$  this length is  $l_0 = \sqrt{\hbar/2m\omega_{\text{osc}}}$ . Reference [4] predicts that for a sufficiently large value of the ratio  $a/l_0$  the mean-field interaction becomes positive allowing

the formation of a stable condensate. A second interest in a strong 1D confinement is the possibility to use a very efficient optical cooling method, sideband cooling [8–13]. This method requires  $l_0 \ll \lambda$  (Lamb-Dicke regime), where  $\lambda$  is the optical wavelength of the cooling transition. For instance, in Ref. [11], 92(5)% of the atoms have been cooled to the ground state in the tightly confined direction. Several trap configurations for achieving 2D gases are under investigation. Many of them are based on far-off-resonance optical dipole traps [14] and evanescent fields near the surface of a dielectric [15,16]. Another common approach is to confine atoms in microwells of a 1D far-detuned optical lattice [8,11,17].

In this paper, we present an implementation of Raman sideband cooling of cesium atoms in an intensity lattice created at the intersection of two far-detuned yttrium aluminum garnet (YAG) laser beams. The cooling method, first studied in Ref. [8], uses Raman transitions between Zeeman substates of  $|F=3\rangle$  and produces an atomic sample polarized in  $|F=3, m=3\rangle$ . 83(5)% of the atoms are accumulated in the ground state of motion in the direction of the lattice. The intensity lattice is vertical but atoms are also weakly confined in the horizontal plane owing to the YAG Gaussian beam intensity profiles. Elastic collisions couple the vertical and horizontal degrees of freedom so that 1D sideband cooling efficiently cools in the three directions [8]. A horizontal temperature  $T_h = 2.8 \mu\text{K} = 0.7\hbar\omega_{\text{osc}}/k_B$  has been obtained, which already corresponds to the condition of a quasi-two-dimensional gas. We show that the cooling efficiency should become exponentially small for  $k_B T < \hbar\omega_{\text{osc}}$  and we propose a dynamical method to reach a lower ratio  $k_B T/\hbar\omega_{\text{osc}}$ . Finally, we address the question of the influence of the strong

---

\*Present address: Institute for Laser Science, University of Electro-Communications, Chofu-city, Tokyo, 182-8585 Japan.

confinement on collisional properties. For this purpose, we measure the rates of thermalization between the strongly and weakly confined degrees of freedom. In the explored temperature range from 4 to 20  $\mu\text{K}$ , our results are compatible with the zero-energy scattering resonance previously observed in weak 3D traps [18–20]. The experimental data also agree with calculations of Ref. [21] that takes into account the quantum character of the particle motion in the strongly confined direction. We propose simple analytical models that reproduce the expected behavior for  $k_B T \gg \hbar \omega_{\text{osc}}$ , and also for  $k_B T \ll \hbar \omega_{\text{osc}}$ , where the 2D character of the particle motion is prominent.

The paper is organized as follows. In Sec. II, we describe the experimental setup and the intensity lattice. Section III recalls the cooling-method principle and gives a detailed account of the geometry we used that is different from that in Ref. [8]. We present independent experimental determinations of the parameters relevant for the cooling. The role of the polarization of the trapping beams for the cooling is discussed in detail. In Sec. IV, the vertical cooling obtained is presented. This cooling is compared with the expected cooling, taking into account several features of our experiment. The role of the polarization of the trapping beam for the cooling efficiency, discussed theoretically in Sec. III, is investigated experimentally. Section V presents cooling of the horizontal motion. In Sec. VI we propose a method to overcome the exponential decrease of the horizontal cooling efficiency as the temperature decreases and we present an experimental implementation of this method. In Sec. VII, we investigate collective effects. First, we report a dependence of the temperature on the number of atoms. Then, we investigate the losses of atoms observed during the long cooling time required for the horizontal cooling. We show that these losses are consistent with the expected losses due to light-assisted exothermic collisions by the repumper beam. Section VII is devoted to the study of collisional properties. After an introduction giving the relevant parameters, the experimental measurements of thermalization times are described in detail. Finally, two calculations give the expected behavior in the two limits  $k_B T \gg \hbar \omega_{\text{osc}}$  and  $k_B T \ll \hbar \omega_{\text{osc}}$ . At high temperature, we perform classical calculation using the Boltzmann equation. At low temperature, simple qualitative arguments show an exponential decrease of the thermalization rate between the horizontal and vertical degrees of freedom. We thus recover the more rigorous calculation of Ref. [21]. This calculation also explains the inhibition of the horizontal cooling when  $k_B T \ll \hbar \omega_{\text{osc}}$ , when sideband cooling is performed only in the vertical direction.

## II. THE FAR-DETUNED TRAP

Our 1D intensity lattice is similar to the one described in Ref. [11]. It is produced at the crossing of two beams of a YAG laser (1.06  $\mu\text{m}$ ), propagating in a vertical plane and making an angle  $\theta_{\text{YAG}} = 52^\circ$  with the horizontal direction. Both beams have linear polarizations as presented in Fig. 1. Each beam has a waist of 100  $\mu\text{m}$  and a power of about 5 W. The YAG laser is far detuned to the red of the  $D1$  and  $D2$  transitions of cesium at 852 nm and 894 nm. The atoms

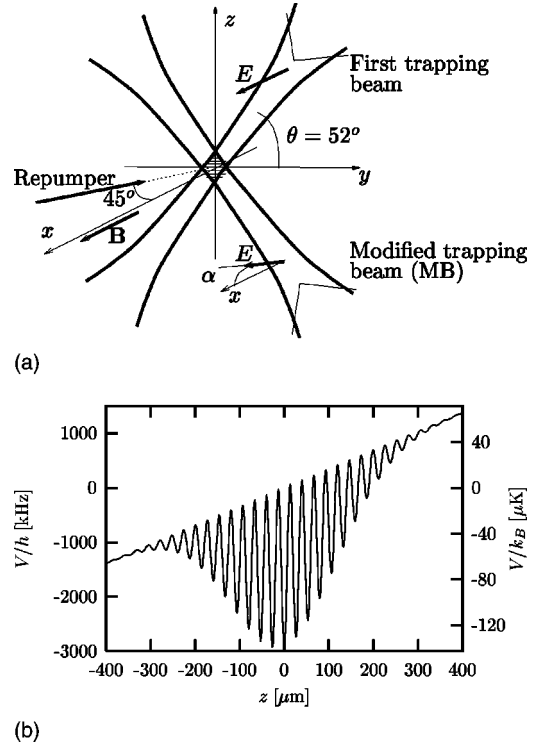


FIG. 1. (a) Laser beam configuration used in sideband cooling of cesium. Atoms are confined in independent horizontal micro-wells resulting from the interference between the two YAG laser beams propagating in the  $y$ - $z$  plane. A weak magnetic field is applied along  $x$ . A repumping beam tuned to  $|6s_{1/2}, F=3\rangle \rightarrow |6p_{3/2}, F'=2\rangle$  propagates in the  $x$ - $y$  plane and makes an angle of  $45^\circ$  with the  $x$  axis. The polarization of one YAG beam is linear along  $x$  and the polarization of the other YAG beam (MB) makes a small angle  $\alpha$  with  $x$ . (b) Trapping potential along  $z$ . For more visibility, the period of the lattice (665 nm) has been increased by a factor 40.

experience a dipole potential proportional to the laser intensity that confines the atoms in regions of maximum intensity. For horizontal polarizations, the interference of the two beams creates a vertical intensity lattice with a period of 665 nm, and the dipole potential is modulated in the vertical direction. The horizontal confinement is provided by the gaussian shape of the YAG beams. The total trap depth is about 140  $\mu\text{K}$ . Tunneling between different microwells is totally negligible for temperatures smaller than 50  $\mu\text{K}$  and the atoms are confined in independent microtraps. In the central microtrap, the vertical oscillation frequency is  $\omega_{\text{osc}}/2\pi = 80$  kHz and the horizontal oscillation frequencies are  $\omega_x/2\pi = 175$  Hz and  $\omega_y/2\pi = 140$  Hz. The spontaneous emission rate at the bottom of the trap is about  $3 \text{ s}^{-1}$ . It leads to a heating rate of 0.38  $\mu\text{K/s}$  that we can neglect in the following experiments. This trap is loaded from a magneto-optical trap as explained in Ref. [11]. About  $2 \times 10^5$  atoms are trapped in a gaussian cloud of rms dimensions  $\sigma_x = 31 \mu\text{m}$ ,  $\sigma_y = 39 \mu\text{m}$ ,  $\sigma_z = 60 \mu\text{m}$ , thus populating about 200 horizontal microtraps. Their temperature is  $\sim 20 \mu\text{K}$ , which corresponds for the vertical motion to a mean vibrational number  $\langle n \rangle = 5.8$ . The vertical oscillation frequency depends on the position in the trap and varies by 15% within

the spatial extension of the cloud.

Using a charged-coupled-device camera, we perform two-dimensional absorption images of the atomic cloud. The probe beam is horizontal and makes an angle of  $45^\circ$  with the plane of the YAG beams. First, an image taken just after switching off the YAG beams gives a measurement of the trap size. Second, an image taken after a free expansion time of the cloud gives access to the velocity distribution in the vertical and horizontal directions in the plane of the camera. This time-of-flight method is detailed in Ref. [22].

The Lamb-Dicke parameter is  $\eta = \sqrt{\omega_{\text{rec}}/\omega_{\text{osc}}} = 0.16$  where  $\omega_{\text{rec}} = \hbar k^2/2m$  is the recoil frequency associated with the cesium D2 transition. This low value enables us to cool the atoms to the ground state of motion in the vertical direction by using sideband cooling methods [9–11,23].

### III. COOLING METHOD

#### A. Principle

We describe here the main elements of the sideband cooling of the vertical motion as developed by Vuletić *et al.* [8]. This cooling uses only Zeeman sublevels of the Cs  $F=3$  hyperfine ground state and produces a sample polarized in  $|F=3, m=3\rangle$ . A magnetic field is applied along the  $x$  axis such that the Zeeman sublevels of  $F=3$  acquire different energy shifts. A repumping laser that is resonant with the transition  $|6s_{1/2}, F=3\rangle \rightarrow |6p_{3/2}, F'=2\rangle$  and which has a polarization with only  $\pi$  and  $\sigma_+$  components, provides a finite linewidth of all Zeeman substates of  $F=3$  except for  $|F=3, m=3\rangle$ . Zeeman states with  $m$  differing by  $\pm 1$  are coupled by a Raman process such that the Raman transition  $|m\rangle \rightarrow |m-1\rangle$  is resonant with the transition that decreases the vibrational quantum number by one. If the Raman coupling and the intensity of the repumping laser are sufficiently small, the motional sidebands  $|m=3, n\rangle \rightarrow |m=2, n'\rangle$  are well resolved and the state  $|m=3, n=0\rangle$  is a quasi-dark state. Its lifetime is limited only by off-resonant Raman transfer and is much longer than that of the other states. In the Lamb-Dicke regime the vibrational energy of the atoms is much larger than the recoil energy. Therefore, the Raman transition to a Zeeman level with  $m < 3$  followed by optical repumping to  $m=3$ , leads on average to a decrease of the atom's energy. Thus by repetition of such cycles, atoms are cooled and accumulate in the quasidark state  $|m=3, n=0\rangle$ . A weak intensity laser tuned to the  $|F=4\rangle \rightarrow |F'=4\rangle$  transition prevents atoms from accumulating in the  $|F=4\rangle$  state after spontaneous emission. The magnetic field is chosen so that the energy of  $|m, n\rangle$  equals the energy of  $|m-1, n-1\rangle$ . The Raman transition is then resonant if the two Raman beams have the same frequency, and in contrast to our previous work [10,11], we simply use the YAG beams themselves to induce the Raman transitions. In order to introduce coupling between different Zeeman levels, the polarization of one of the beams is slightly modified from the linear horizontal polarization (see Sec. III C).

#### B. Repumping beam

The repumping beam tuned to the  $|F=3\rangle \rightarrow |F'=2\rangle$  transition of the D2 line propagates in the  $x$ - $y$  plane and makes

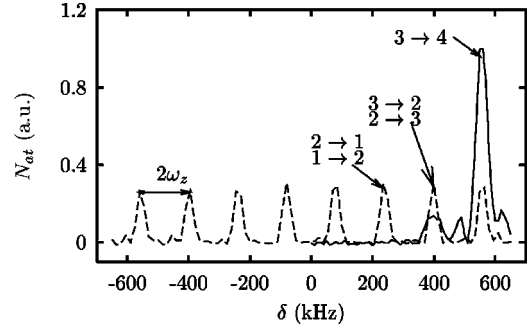


FIG. 2. Number of atoms transferred to the hyperfine ground state  $|F=4\rangle$  by a two-photon Raman pulse as a function of the detuning of the two-photon transition from 9.192 631 770 GHz. The Raman beams propagate in the same direction in order to avoid change of vibrational state during the transfer. The labels indicate the various  $|F=3, m\rangle \rightarrow |F=4, m'\rangle$  transitions. Dashed line, unpolarized atoms; solid line, atoms polarized by a 3.6 ms repumping laser pulse with an intensity of  $0.3I_{\text{sat}}$ . The resulting polarization exceeds 90%.

an angle of  $45^\circ$  with the  $x$  axis. With respect to the axis of the magnetic field, the total intensity of the beam  $I$  splits in  $I/3$  for the  $\pi$  polarization (i.e., along the axis of the magnetic field), and  $2I/3$  for the  $\sigma^+$  polarization. The population of the atoms in each of the Zeeman sublevels of  $F=3$  is measured via frequency selective Raman transitions to  $|F=4\rangle$ . For this purpose we use two Raman beams with frequencies differing by about 9.2 GHz as explained in Ref. [24].

With this method we optimize the parameters of the repumping beam in the absence of Raman coupling between Zeeman sublevels i.e. with parallel linear polarizations of the YAG beams (see Sec. III C). We can measure both the polarization time constant and the steady-state polarization. With our experimental precision, the equilibrium population in  $|m=3\rangle$  deduced from data such as in Fig. 2 is between 90% and 100%. We then deduce an intensity for the  $\sigma_-$  component of the repumping laser smaller than 3% of the  $\pi$  intensity. The measured  $1/e$  polarization time of an initially unpolarized sample is  $10 \mu\text{s} \times I_{\text{sat}}/I$  at small intensities. The calculated lifetime  $\Gamma'^{-1}$  of the state  $|m=2\rangle$  is  $0.8 \mu\text{s} I_{\text{sat}}/I$ . The optical density of our sample is about 2 and we have seen no influence of the number of atoms on the polarization time constant and on the equilibrium polarization. This means that we see no effect of reabsorption of photons on the polarization of the sample.

#### C. Polarization of the YAG beams

The YAG detuning is much larger than the hyperfine splittings of the  $6s_{1/2}$  and  $6p_{3/2}$  states. Hence, if the two YAG beams are linearly polarized along  $x$ , there is no coupling between different Zeeman sublevels. The light-shift operator is scalar (proportional to the identity operator) and all Zeeman substates see the same YAG potential [14]. Raman coupling between different Zeeman levels is obtained by introducing, for one of the trapping beams (called MB), a small component of polarization  $X^0$  orthogonal to the horizontal one. All Zeeman sublevels still share a common potential

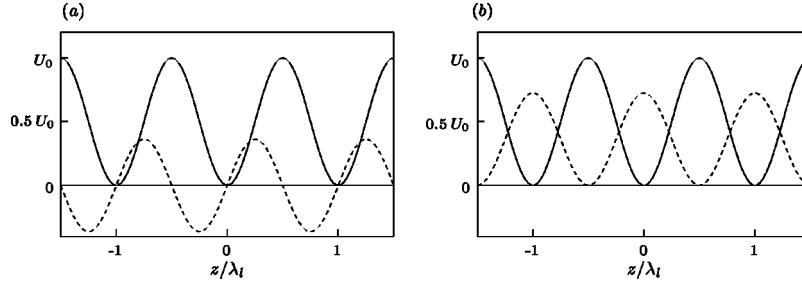


FIG. 3. Raman coupling  $V(z)$  (dashed line) between  $|F=3, m=3\rangle$  and  $|F=3, m=2\rangle$  as a function of the vertical position of the atom. (a) corresponds to a linear polarization of the MB making an angle of  $20^\circ$  with the horizontal direction and (b) corresponds to a polarization of the MB with the same proportion of horizontal polarization but with a relative phase of  $\pi/2$  between the two polarizations. The solid lines depict the dipole potential “seen” by the atoms, the potential being chosen 0 at the bottom of the microwells. For better visibility, we have plotted  $80 \times V(z)$ .

energy and levels  $|m, n\rangle$  and  $|m-1, n-1\rangle$  are degenerate for any  $m \in [-2, 3]$  and vibrational level  $n > 0$ . Raman transfers enable a change of the vertical motion. This corresponds to absorption from one beam and stimulated emission into the other beam. Due to an interference between the two different processes, at the bottom of a microtrap the Raman coupling depends on the relative phase between the component of horizontal polarization and the component along  $X^0$ . The coupling is even in  $z$  for a phase difference of  $\pi/2$  (most elliptical polarization of the MB) but odd for a zero phase difference (linear polarization of the MB) as depicted in Fig. 3. Thus, due to the parity properties of the vibrational states, linear polarization of the MB induces the maximum coupling between neighboring vibrational level whereas a phase difference of  $\pi/2$  between the polarization components induces a coupling only between vibrational levels of the same parity. In the experiment, the relative phase between the two polarization components of the MB is controlled by an adjustable retardation wave plate. For a linear polarization of the MB making an angle  $\alpha$  with respect to  $0x$  (see Fig. 1), the coupling between  $|m=3, n\rangle \rightarrow |m=2, n-1\rangle$  is

$$\begin{aligned} V &= \frac{\sqrt{6}}{24} \eta U_0 \Delta_{\text{YAG}} \left( \frac{1}{\Delta_1} - \frac{1}{\Delta_2} \right) \sin(\alpha) \sin(\theta_{\text{YAG}}) \sqrt{n}, \\ &= V_R \sqrt{n}, \end{aligned} \quad (3.1)$$

where  $\Delta_1$  ( $\Delta_2$ ) is the detuning of the YAG beams with respect to the Cs  $D_1$  ( $D_2$ ) line,  $\Delta_{\text{YAG}} = \Delta_1/3 + 2\Delta_2/3$  and  $U_0 = 4(E_0 d_0)^2 / \Delta_{\text{YAG}}$  is the depth of the trap with linear polarizations. In this formula, only the component of order 1 in  $\eta$  has been retained, which is a good approximation in our situation where  $\eta = 0.16$ . For an angle  $\alpha = 20^\circ$ , the calculated Rabi frequency of the coupling  $|m=3, n=1\rangle \rightarrow |m=2, n=0\rangle$  is

$$\Omega_R = 2 \frac{V_R}{\hbar} = 2\pi \times 6 \text{ kHz}. \quad (3.2)$$

In order to measure the coupling due to the YAG beams, we first polarize the atoms in  $|F=3, m=3\rangle$  by an intense repumping pulse. We then measure the time evolution of the  $|F=3, m=3\rangle$  population using a Raman transition to  $|F=4, m=4\rangle$  as in Fig. 2 (see also Ref. [24]). Figure 4 gives

the evolution of the population in  $|F=3, m=3\rangle$ . The magnetic field for this experiment is chosen so that the levels  $|m=3, n\rangle$  and  $|m=2, n-1\rangle$  are degenerate and the angle of polarization of MB is  $\alpha = 20^\circ$ . We observe a damped oscillation. A damping with a time constant  $\tau \approx \sqrt{\hbar \omega_{\text{osc}} / (k_B T)} \Omega_R^{-1}$  is expected as the coupling  $|m=3, n\rangle \rightarrow |m=2, n-1\rangle$  is proportional to  $\sqrt{n}$ . For a temperature of  $26 \mu\text{K}$ , we expect  $\tau \approx 0.4 \Omega_R^{-1}$ . The Raman coupling, averaged over the population of the vibrational states, is obtained by fitting the first  $40 \mu\text{s}$  of the oscillation with a sine function of amplitude 1. We obtain a Rabi frequency of 5 kHz in reasonable agreement with Eq. (3.2). In this analysis we have supposed that all atoms contribute to the oscillations. However, this is not strictly the case. First atoms in  $|m=3, n=0\rangle$  are not transferred to  $|m=2\rangle$ . Second, atoms far from the center of the trap have a vertical oscillation frequency that differs from the central one. When the difference exceeds  $\sim 5$  kHz, the coupling is no longer perfectly resonant. Both of these effects would lead to a Rabi frequency slightly higher than the measured one, 5 kHz.

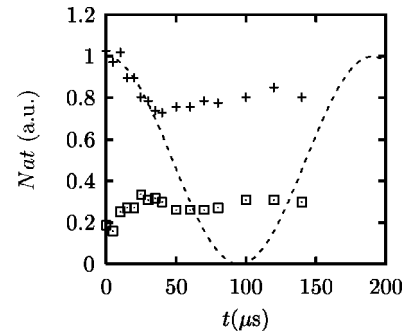


FIG. 4. Experimental determination of the YAG coupling  $|F=3, m=3, n\rangle \rightarrow |F=3, m=2, n-1\rangle$ . The atoms are previously polarized in  $|F=3, m=3\rangle$  by a strong pulse of the repumping beam. Crosses, evolution of the number of atoms transferred from  $|F=3, m=3\rangle$  to  $|F=4, m=4\rangle$  as a function of the delay time of the Raman probe pulse; dashed line, fit of the first  $40 \mu\text{s}$  with a sine function of amplitude 1; squares, number of atoms transferred to  $|F=4, m=2\rangle$  and  $|F=4, m=3\rangle$  on the transitions  $|F=3, m=3\rangle \rightarrow |F=4, m=2\rangle$  and  $|F=3, m=2\rangle \rightarrow |F=4, m=3\rangle$  (see Fig. 2 and Ref. [24]). We deduce a Rabi frequency  $\Omega_R \approx 5$  kHz.

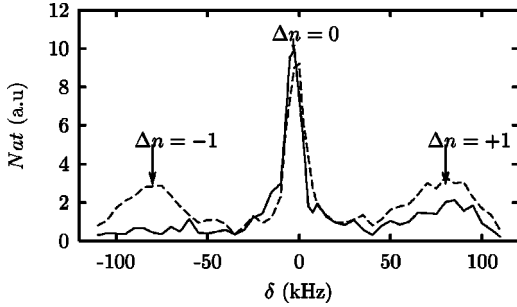


FIG. 5. Number of atoms transferred to the hyperfine ground state  $|F=4\rangle$  by a two-photon Raman pulse as a function of the detuning of the two-photon transition from 9.192 631 770 GHz. The two Raman beams are counterpropagating in order to enable change of vibrational level. The magnetic field has been turned off before the Raman pulse so that all the transitions  $|F=3,m\rangle \rightarrow |F=4,m'\rangle$  are degenerate. Dashed line, Raman spectrum before cooling; solid line, Raman spectrum after 20 ms cooling. The labels indicate the change of vibrational level during the transfer. After cooling, the red sideband corresponding to a decrease of the vibrational level by 1 has disappeared. This indicates that nearly all atoms are in the motional ground state  $|n=0\rangle$ .

#### IV. COOLING OF THE VERTICAL MOTION

##### A. Measured temperature

The smallest vertical temperature we achieved with this sideband cooling method is about  $0.56\hbar\omega_{\text{osc}}$ , which corresponds to about 83(5)% of the atoms accumulated in the ground state of motion. This temperature is measured either by time-of-flight absorption imaging or by using a Raman transition from  $|F=3,m=3\rangle$  to  $|F=4,m=4\rangle$  with counterpropagating beams. The vibrational sidebands are resolved (Fig. 5) and from the height of the red sideband we deduce the population of the  $n>0$  vibrational states [11]. Both measurements are in agreement at the 5% level.

The measured  $1/e$  cooling time constant is 2.5 ms. Such a cooling is obtained for an intensity of the repumping beam of  $2.4 \times 10^{-2} I_{\text{sat}}$ , where  $I_{\text{sat}} = 1.1 \text{ mW/cm}^2$  is the saturation intensity. This beam intensity corresponds to a calculated energy width of  $|m=2\rangle$   $\hbar\Gamma' = h \times 4.8 \text{ kHz}$ . The MB has a linear polarization with  $\alpha = 20^\circ$  corresponding to a Raman coupling  $|m=3,n=1\rangle \rightarrow |m=2,n=0\rangle$  of  $h \times 2.5 \text{ kHz}$ . This ground-state population of 83(5)% is slightly lower than the value [92(5)%] we previously obtained with sideband Raman cooling of unpolarized atoms involving the two hyperfine states  $|F=3\rangle$  and  $|F=4\rangle$  [11].

##### B. Discussion

The expected equilibrium temperature can easily be calculated in the Lamb-Dicke regime where  $\eta \ll 1$  if the equilibrium is set by nonresonant excitation from  $|m=3,n=0\rangle$  to  $|m=2\rangle$ , [25–27]. The following simple argument gives the equilibrium temperature in the limit where the Raman coupling is much smaller than the lifetime  $\Gamma'$  of  $|m=2\rangle$ . For  $\eta \ll 1$ , we can neglect any change of vibrational level during the repumping process. Furthermore, the Raman transfer inducing a change of the vibrational level by  $k \geq 2$ , of order  $\eta^k$ ,

can be neglected compared to the Raman coupling with a change of vibrational level by 1. Thus, the two processes in competition that define the equilibrium are the process  $|m=3,n=0\rangle \rightarrow |m=2,n=1\rangle \Rightarrow |m=3,n=1\rangle$  and the resonant process  $|m=3,n=1\rangle \rightarrow |m=2,n=0\rangle \Rightarrow |m=3,n=0\rangle$ , where  $\Rightarrow$  indicates optical pumping. Note that the Raman transfer  $|m=3,n=0\rangle \rightarrow |m=2,n=0\rangle$  is not allowed with linear polarization of the MB. In the limit where the Raman coupling is much smaller than the energy width  $\Gamma'$  of  $|m=2\rangle$ , equaling the rates of these two processes gives a relative population of  $|m=3,n=1\rangle$  of  $(\Gamma'/4\omega_{\text{osc}})^2$ . The expected cooling rate is  $\Gamma_{\text{cool}} = \Omega_R^2/\Gamma'$ . With our experimental parameters, this leads to a temperature of about  $0.12\hbar\omega_{\text{osc}}$  (population of  $|m=3,n=1\rangle$  of 0.0002), a factor of 4.6 smaller than the obtained temperature. The predicted cooling rate is  $3 \times 10^4 \text{ s}^{-1}$  ( $1/e$  cooling time of 30  $\mu\text{s}$ ).

We discuss now some possible sources of discrepancy between this simple model and the experiment, although we find that they are not sufficient to explain the observed equilibrium temperature. First, the resonance of the transition  $|m=3,n=1\rangle \rightarrow |m=2,n=0\rangle$  is not fulfilled for all the atoms. Indeed, the vertical oscillation frequency of the atoms, which depends on their position in the trap, spreads over about 15% of the central 80 kHz frequency. If the transition is detuned by  $\delta > \Gamma'$ , the expected steady-state population of  $|m=3,n=1\rangle$  is  $[\delta/(2\omega_{\text{osc}})]^2$ . For  $\delta = 0.15\omega_{\text{osc}}$ , this population is only 0.005, still smaller than the measured one. However, the cooling rate is significantly modified by this effect; for instance, it is reduced by a factor 36 for a detuning of  $0.15\hbar\omega_{\text{osc}} = 12 \text{ kHz}$ . Thus, the spread of oscillation frequencies is likely to be the cause of the long cooling time observed. Second, nonresonant Raman transfer is not the only process causing a departure from  $|m=3,n=0\rangle$ . Indeed, a component of  $\sigma_-$  polarization of the repumping beam would excite atoms in  $|m=3\rangle$ . The measurement of the steady-state polarization without Raman coupling shows that the excitation rate of  $|m=3\rangle$  is smaller than  $0.01\Gamma'$ . The heating produced by this excitation is smaller than or on the order of  $0.01E_{\text{rec}}\Gamma'$ . For atoms resonant with the  $|m=3,n=1\rangle \rightarrow |m=2,n=0\rangle$  transition, this would lead to a steady-state population in the excited vibrational states of 0.003 much smaller than the measured one. However, atoms detuned by 12 kHz (the typical width of the distribution of oscillation frequency in the cloud) experience a smaller cooling rate and, therefore, the steady-state population of excited states increases to about 1% for these atoms.

Finally, heating due to multiple photon scattering within the cloud is likely to bring a negligible contribution to the observed mean vibrational number because the optical density is only 2.

##### C. Effect of the polarization of the MB

The Raman transfer  $|m=3,n\rangle \rightarrow |m=2,n-1\rangle$  is resonant when the Zeeman splitting is equal to the vibrational energy. Figure 6(a) shows this resonant behavior of the cooling as a function of magnetic field. For a Zeeman splitting equal to  $2\omega_{\text{osc}}$ , a transfer  $|m=3,n\rangle \rightarrow |m=2,n-2\rangle$  is resonant. But with a linear polarization of the MB, such a transfer is for-

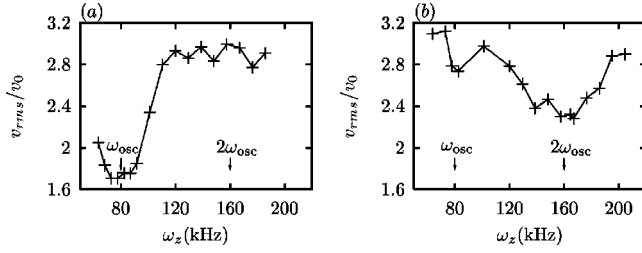


FIG. 6. rms width of the vertical velocity distribution obtained after 30 ms of cooling as a function of the Zeeman splitting between adjacent Zeeman levels.  $v_0 = \sqrt{\hbar m \omega_{\text{osc}}/2}$  is the rms width of the vibrational ground state. The polarization of the MB is linear in (a) and elliptical in (b).

bidden (no coupling between levels of same parity as shown in Fig. 3 of Sec. III C). In contrast, when we choose an elliptical polarization of the MB, cooling on the second sideband is observed [Fig. 6(b)]. This cooling is weak because the Raman coupling is very small for a small Lamb-Dicke parameter. In this case, as expected, almost no cooling is observed on the first sideband.

### V. COOLING THE HORIZONTAL MOTION

To cool the horizontal degrees of freedom with the vertical sideband cooling, a transfer of energy from horizontal to vertical motion is needed. This transfer can be provided by collisions between atoms and efficient cooling of the three degrees of freedom has been demonstrated in Ref. [8]. In our experiments, after 1 s of vertical sideband cooling, the horizontal temperature drops from  $T_h = T_v = 13 \mu\text{K}$  to  $T_h = 2.7 \mu\text{K}$  and  $T_v = 1.6 \mu\text{K}$  as presented in Fig. 7. For these data, the cooling rate of the vertical motion is much higher than the horizontal one. The intensity of the repumping beam is decreased to about  $2.5 \times 10^{-3} I_{\text{sat}}$ , which is about 10 times smaller than the power that leads to the most effective cooling of the vertical motion. This is due to the heating of the horizontal motion experienced by the atoms even after reaching the steady state of the vertical motion. Indeed, the steady

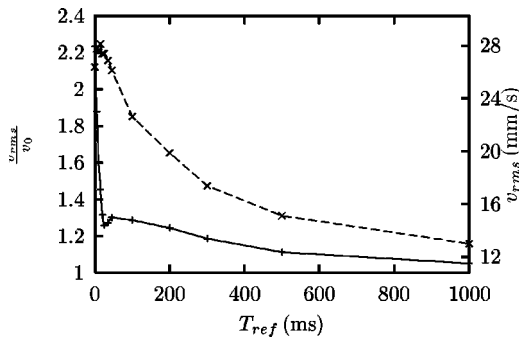


FIG. 7. Evolution of the rms velocity width in the vertical (+) and the horizontal ( $\times$ ) directions as a function of the cooling time.  $v_0$  is the width of the ground state of motion in the vertical direction. Note, at very short cooling time, the initial increase of the velocity spread in the horizontal direction. It is due to the spontaneously emitted photons required for the sideband cooling of the vertical motion.

state of the vertical cooling is an equilibrium between heating processes like excitation by the  $\sigma_-$  component of the repumper and the cooling itself. Spontaneous photons are emitted at a rate proportional to the intensity of the repumping laser and the spontaneous photons emitted in the horizontal directions are responsible for a heating of the horizontal motion. To achieve a heating smaller than the cooling rate due to the collisions, the power of the repumper should thus be small enough. Figure 7 also indicates that the cooling in the vertical direction is affected by the energy in the horizontal planes since the rms velocity in the vertical direction tends slowly to the ground state rms velocity as the horizontal temperature decreases.

In the horizontal plane, we could achieve a temperature  $T = 2.8 \mu\text{K}$  ( $k_B T = 0.7 \hbar \omega_{\text{osc}}$ ) which corresponds to a mean kinetic energy per degree of freedom of  $1.3 \hbar \omega_{\text{osc}}/4$ . For such a low horizontal temperature, the energy transfer between the horizontal and vertical degrees of freedom due to the collisions is very inefficient. Indeed, we explain in Sec. VIII E, that for small horizontal temperatures, the rate of energy transfer due to collisions goes down exponentially with a factor  $\exp(-2 \hbar \omega_{\text{osc}}/(k_B T))$  as the temperature decreases. This factor, which is 0.5 for the typical initial horizontal temperature ( $k_B T = 3 \hbar \omega_{\text{osc}}$ ), is only 0.06 for the final temperature. Thus, even if the vertical equilibrium temperature of the sideband cooling  $T_{\text{eq}}$  is much smaller than  $\hbar \omega_{\text{osc}}$ , we expect that the rate of the horizontal cooling decreases exponentially as  $k_B T < \hbar \omega_{\text{osc}}$ . Small external sources of heating would then cause the horizontal cooling to stop before  $T_{\text{eq}}$  has been reached. This inhibition of the coupling between the vertical and horizontal degrees of freedom for temperatures smaller than  $\hbar \omega_{\text{osc}}$  is an important limitation of 3D cooling using 1D sideband cooling and collisions.

The highest phase-space density obtained is  $n \lambda_{\text{DB}}^3 = 1.3 \times 10^{-3}$ , where  $\lambda_{\text{DB}} = \hbar \sqrt{2 \pi / m k_B T}$  is the de Broglie wave-length and  $n$  is the peak atomic density. This is obtained after cooling to a temperature  $k_B T_h = k_B T_v = 4.3 \mu\text{K}$  with about 450 atoms per microtraps at a peak density  $n = 4 \times 10^{12} \text{ atoms/cm}^3$ .

### VI. A METHOD TO COOL FURTHER: CHANGE OF POLARIZATION ANGLE $\alpha$

To overcome the decrease of the cooling efficiency of the horizontal motion as the temperature decreases, we changed the parameters of the trap during the sideband cooling. More precisely, the ratio of the horizontal to the vertical oscillation frequencies is increased. Thus, if the change is done adiabatically with respect to the oscillation of the atoms, the ratio of the energy of the horizontal motion to the energy of the vertical motion will increase. More pairs of colliding atoms will then have a horizontal energy sufficient to populate the excited vibrational states after the collision. This change is realized by increasing the angle  $\alpha$  of the polarization of the MB with respect to the horizontal direction, using a retardable wave plate on a time scale of about 10 ms. With a large angle  $\alpha$ , the contrast of the interferences between the two trapping beams is reduced leading to a decrease of the vertical oscillation frequency by a factor  $\sqrt{\cos(\alpha)}$ . Because the

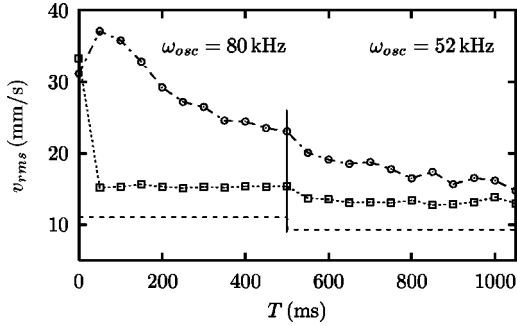


FIG. 8. Two-step cooling with a decrease of the vertical oscillation frequency after 500 ms. Squares, rms velocity width along  $z$ ; circles, rms velocity width along  $x$ . The dashed straight lines give the rms velocity width of the ground state of motion in the vertical direction.

depth of the trap is reduced when  $\alpha$  increases, the horizontal oscillation frequencies are also reduced by a factor  $\sqrt{[1 + \cos(\alpha)]/2}$  that is smaller than the previous factor  $\sqrt{\cos(\alpha)}$ .

Experimentally, we decrease the vertical oscillation frequency from  $\omega_{z_1} = 80(3)$  to  $\omega_{z_2} = 53(2)$  kHz, (decrease by a factor 0.67), corresponding to  $\alpha$  going from  $29^\circ$  to  $63^\circ$ . The horizontal oscillation frequencies decrease only by a factor  $\omega_{x_2}/\omega_{x_1} = 0.88$ . At 53 kHz, sideband cooling still works well, after the corresponding change of the magnitude of the magnetic field. We also found that a decrease of the repumping power by a factor 3.3 was required. Figure 8 gives the time evolution of the horizontal and vertical velocity distributions before and after the change of the vertical oscillation frequency. More efficient cooling after the change of the oscillation frequency is clearly visible.

If we assume that the cooling for a large value of  $\alpha$  produces  $k_B T_h = \beta \hbar \omega_z$ , when returning the polarization to its original value the final horizontal temperature is given by  $k_B T_h / (\hbar \omega_{z_1}) = \beta (\omega_{x_1} / \omega_{x_2}) (\omega_{z_2} / \omega_{z_1})$ . In this way, we could produce a horizontal temperature that could not be obtained by cooling only with  $\omega_{z_1}$  because of the decoupling between horizontal and vertical motions at low temperature.

## VII. DEPENDENCE OF THE TEMPERATURE ON THE NUMBER OF ATOMS AND ATOM LOSSES

Dependence of the measured temperature with the number of atoms has been observed. Both the vertical and the horizontal temperatures achieved after 500 ms of cooling are found to increase with the final number of atoms  $N$  about as  $dT/dN \approx 4 \times 10^{-5} \mu\text{K}/\text{atom}$  in the explored range  $N = 40 \times 10^3 - 90 \times 10^3$ . However, the cooling efficiency of the horizontal motion is expected to increase with  $N$  as the collision rate increases. The positive slope  $dT/dN$  can be due to heating by the reabsorption of spontaneous photons or by exothermic light-assisted collisions.

We also found that the sideband cooling is accompanied by losses of atoms: about 50% of the atoms have been lost in the first 500 ms of the cooling presented in Fig. 7. The corresponding loss rate of about  $1.0(1) \text{ s}^{-1}$  is significantly larger

than the measured loss rate due to collisions with the background gas [ $0.4(1) \text{ s}^{-1}$ ].

We believe that these losses are due to exothermic collisions assisted by the repumper light [28]. However, a clear dependence of the loss rate on the density of atoms characteristic of such a two-body loss mechanism could not be obtained. Indeed, due to the dependence of the temperature on the number of atoms, only small density changes have been achieved and no conclusive results could be deduced.

For the depth of our trap (about  $140 \mu\text{K}$ ), the dominant inelastic light-assisted process is radiative escape [29]. We give below an estimate of the loss rate due to this process in our experiments, based on earlier calculations made by Julienne and Vigué [30]. The loss rate can be written  $K n_{\text{ex}}$ , where  $n_{\text{ex}}$  is the density of excited atoms. For a temperature of  $100 \mu\text{K}$ , a trap depth of 1 K, and a detuning of the laser of  $-\Gamma$ ,  $K \approx 0.2 \times 10^{-11}$  [30]. Because  $K$  scales with the depth  $U$  of the trap as  $U^{5/6}$  [30], we expect  $K$  to be bigger by a factor  $1.7 \times 10^3$  in our trap. As the repumping beam in our experiments is on resonance, we may expect a slight change of the factor  $K$ , that we neglect for this estimate. The density of excited atoms after the first 10 ms of strong vertical cooling, is mainly determined by excitation of the atoms in  $|m=3\rangle$  due to the  $\sigma_-$  component of the repumper. With the experimental parameters and taking a component of bad polarization of the repumping beam of 5%,  $n_{\text{ex}}$  is about  $n \times 0.6 \times 10^{-4}$ , where  $n$  is the total density of atoms. With a mean density  $n = 5 \times 10^{11} \text{ at}/\text{cm}^3$ , the estimated loss rate is then  $0.15 \text{ s}^{-1}$ . This loss rate is of the same order of magnitude as the measured one. We note that, contrary to our findings, no atom losses were observed in Ref. [8], although the density achieved in [8] was three times higher than ours.

## VIII. COLLISIONAL PROPERTIES

### A. Introduction

In the ground state of motion in the vertical direction, atoms are confined in a Gaussian distribution with rms size  $l_0 = 20 \text{ nm}$ . On the other hand, the scattering length of cesium atoms that characterizes the collisional properties at low energy is, for the  $|F=3, m=3\rangle$  state, negative with an absolute value larger than  $60 \text{ nm}$  [6,20,23] (The most recent calculations of Ref. [6], based on the analysis of several Feshbach resonances of Ref. [23] give  $a = -138 \text{ nm}$ .) An interesting question is then: are the collisional properties altered by the strong 1D confinement as compared to the free-space case? With such a high absolute value of the scattering length, for the temperatures in our experiments, the collisional cross section for free atoms reaches its maximum allowed value of  $8\pi/k^2$  where  $k$  is the wave vector of the relative motion. This resonance behavior has been observed in weak traps by measuring thermalization times as a function of temperature [18–20]. The quantity  $1/(n\nu T_{\text{therm}})$ , where  $n$  is the density of atoms, which is expected to be proportional to the typical collision cross section  $\sigma$ , was found proportional to  $1/T$ . This was interpreted as a zero-energy resonance and  $\sigma$  was found equal to  $8\pi/k^2$  between 5

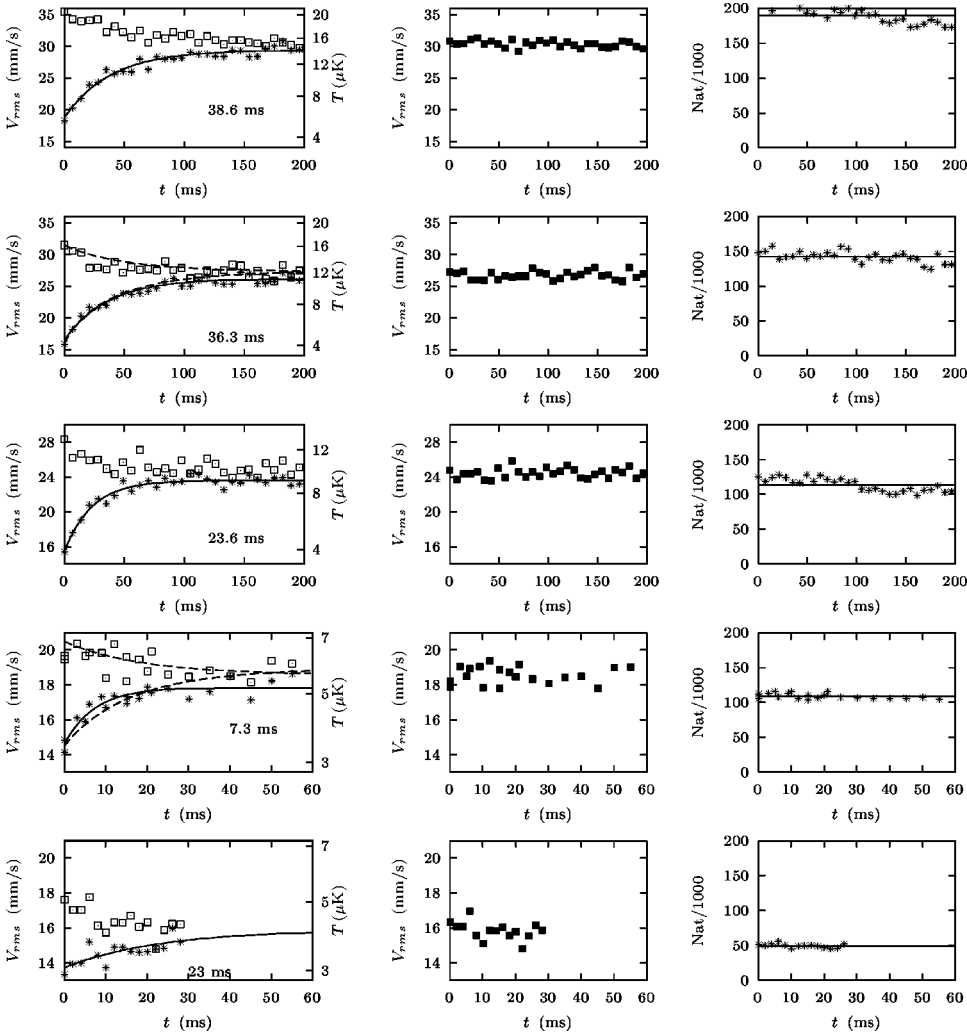


FIG. 9. Free evolution of the rms width of the velocity distribution along the vertical direction (stars,  $v_z$ ) and along the horizontal direction  $x$  (open squares,  $v_x$ ), after switching off the sideband cooling for different initial conditions. The solid line is an exponential fit of the evolution of  $v_z$  and the  $1/e$  time is noted on the graphs. On the second and fourth graphs, the evolutions predicted by the calculations of Petrov and Shlyapnikov for the same initial velocity distribution and for the same initial density are shown in dashed lines [21]. The second column shows  $\sqrt{(v_z^2 + 2v_x^2)/3}$ , the velocity corresponding to the mean kinetic energy per degree of freedom. The third column gives the number of atoms. Each point is the average of 20 successive measurements.

and  $60 \mu\text{K}$ . We give below an analytical derivation, in the classical limit ( $k_B T \gg \hbar \omega_{\text{osc}}$ ), of the thermalization time  $T_{\text{therm}}$ .

In our trap, at temperatures much larger than the vibrational energy  $\hbar \omega_{\text{osc}}$ , we expect the collisions to be 3D collisions. Indeed, in this case, the motion of the atoms can be understood as oscillations of wave packets of quite well-defined wave vector  $k$ . The collision of two wave packets occurs on a spatial scale  $1/k$  (square root of the cross section). For the typical wave vector  $k = \sqrt{mk_B T}/\hbar$  and for  $k_B T \gg \hbar \omega_{\text{osc}}$ , this spatial scale is much smaller than the spatial amplitude of the oscillation  $\hbar k/(m\omega_{\text{osc}})$ .

On the other hand, at temperatures  $k_B T \leq \hbar \omega_{\text{osc}}$ , Petrov and Shlyapnikov predict drastic changes of the collisional and thermalization properties, such as a change of the sign of the scattering length [4] and an exponentially vanishing rate of the thermalization between the strongly confined motion and the transverse ones [21]. As a test of these possible changes we have investigated the zero-energy resonance and searched for confinement-induced modifications of the thermalization rates at various temperatures.

## B. Measurements

A situation out of thermal equilibrium is easily produced by the vertical sideband cooling method described above. As

the cooling rate of the vertical motion is much larger than the collision rate, most of the atoms are quickly cooled to the ground state of the vertical motion, while the horizontal motion is cooled more slowly. At any cooling time, the horizontal temperature is higher than the vertical one. If the vertical cooling is stopped, the cloud of atoms relaxes towards equilibrium. We then measure the time evolution of the widths of the velocity distributions along the vertical and horizontal directions. We checked that this relaxation is indeed due to collisions by measuring thermalization times for different numbers of atoms— $T_{\text{therm}}$  is found to be inversely proportional to the number of trapped atoms.

The initial horizontal temperature is varied by changing the time duration of the sideband cooling phase before measuring the thermalization time constant. We could thus measure thermalization times for initial horizontal temperatures varying from  $20 \mu\text{K}$  to  $4 \mu\text{K}$ . The maximum temperature is limited by the depth of the trap. Figure 9 presents many measurements of thermalizations corresponding to various initial temperatures. As the absorption imaging is destructive, each point in Fig. 9 corresponds to a different experimental cycle lasting about 2 s. Fluctuations in the number of atoms for a given cooling time are about 2%. We check that  $2E_{c_x} + E_{c_z}$ , where  $E_{c_x}$  and  $E_{c_z}$  are the mean kinetic energies along

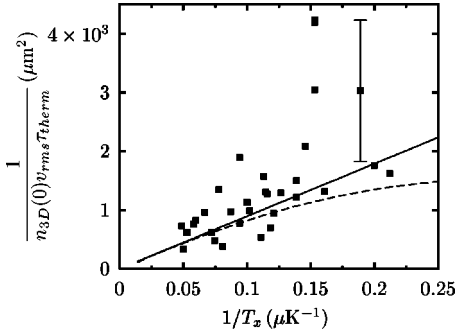


FIG. 10. Comparison between experimental results of thermalization and theoretical calculations in the temperature interval (4, 20  $\mu$ K). The solid line corresponds to the three-dimensional behavior [Eq. (8.9)]. The dashed line results from the quantum calculations of Petrov and Shlyapnikov (see text). A typical error bar for a point at low temperature is shown.

the vertical and horizontal axis of the camera, is conserved to within about 5% (see Fig. 9). This behavior is expected if the thermalization time is much larger than the oscillation time. Indeed, in this case, we expect that the energy is always equally distributed between the potential and kinetic energy and that the horizontal velocity distribution stays isotropic.

### C. Results

Figure 10, presents, as a function of temperature, the quantity  $1/(n_{3D}v_{\text{rms}}T_{\text{therm}})$ , where  $v_{\text{rms}}$  is the initial (i.e., at the beginning of the thermalization) rms width of the horizontal motion and  $T_{\text{therm}}$  is the  $1/e$  thermalization time deduced from an exponential fit to the evolution of the vertical velocity width.  $n_{3D}$  is the initial mean density seen by an atom. It is averaged over the different vertical microplanes and the population of the different microplanes is deduced from the measured Gaussian vertical distribution of atoms and the lattice period. Furthermore we assume that the temperature is identical in all microplanes.  $n_{3D}$  is then deduced from the temperature measurement and from the vertical and horizontal oscillation frequencies. The horizontal oscillation frequencies (of the order of 175 and 140 Hz) are measured through the heating of the atomic cloud produced by parametric drive [31] with a precision of about 5%.

The straight line in Fig. 10 corresponds to the expected behavior when  $k_B T \gg \hbar \omega_{\text{osc}}$ . It results from the 3D *classical* calculation presented below, where the scattering resonance is assumed but where the quantization of the vertical motion is not taken into account. Within our experimental accuracy and for the explored 4–20  $\mu$ K temperature range, we have seen no modification of the scattering resonance induced by the strong 1D confinement: our measurements are compatible with the *classical* calculation. They are also compatible with the full quantum calculation performed by Petrov and Shlyapnikov [21] (dashed line in Fig. 10), which departs significantly from the *classical* calculation only for temperatures much below 4  $\mu$ K. The quantum calculation assumes an oscillation frequency of 80 kHz and a scattering length  $a$  of  $-60$  nm. As this scattering length is already larger than the size of the ground-state wave function, the calculation

does not differ much from the  $|a| = \infty$  case. It also shows that for  $k_B T \ll \hbar \omega_{\text{osc}}$  the thermalization time is expected to increase exponentially as

$$T_{\text{therm}} = \frac{9m}{64\hbar} \frac{1}{\bar{n}_{2D}} e^{\hbar \omega_{\text{osc}}/k_B T}. \quad (8.1)$$

As we will show below, this behavior can also be understood assuming that the scattering resonance is still valid but taking into account the discrete structure of the vibrational energy in the vertical direction and parity conservation during the collision.

### D. Classical calculation of $T_{\text{therm}}$

We propose here a calculation of the thermalization time in the limit  $k_B T \gg \hbar \omega_{\text{osc}}$ . In this condition, the motion of the atoms can be treated classically. The collisions are the same as for free atoms and can be considered as “pointlike” because the extension of the cloud is much bigger than the square root of the typical crosssection. Finally we assume that  $\sigma = 8\pi/k^2$ .

We are interested in the description of the thermalization between the horizontal motion and the vertical one. Thus we consider the evolution of

$$\Delta E = E_z - \frac{1}{2} E_\rho, \quad (8.2)$$

where  $E_z$  and  $E_\rho$  are the kinetic energies of the vertical and horizontal motions.  $\Delta E$  vanishes at thermal equilibrium. If we neglect the anharmonicity of the trapping potential, only collisions can change  $\Delta E$ . A collision where two atoms of velocities  $\mathbf{v}_1$  and  $\mathbf{v}_2$  end up with the respective velocities  $\mathbf{v}_3$  and  $\mathbf{v}_4$  changes  $\Delta E$  by

$$\delta_{12 \rightarrow 34} = \frac{1}{2} m [v_{z_3}^2 + v_{z_4}^2 - v_{z_1}^2 - v_{z_2}^2 - \frac{1}{2}(v_{\rho_3}^2 + v_{\rho_4}^2 - v_{\rho_1}^2 - v_{\rho_2}^2)], \quad (8.3)$$

where the indices  $\rho$  and  $z$  refer, respectively, to the horizontal and vertical component of the velocity. Energy conservation implies

$$\delta_{12 \rightarrow 34} = \frac{3}{2} \frac{1}{2} m (v_{z_3}^2 + v_{z_4}^2 - v_{z_1}^2 - v_{z_2}^2). \quad (8.4)$$

If we note  $f(\mathbf{r}, \mathbf{v})$  the phase-space distribution, the rate of change of  $\Delta E$  is

$$\frac{d\Delta E}{dt} = \int d^3 \mathbf{r} \frac{1}{4} \int d^3 \mathbf{v}_1 d^3 \mathbf{v}_2 d^3 \mathbf{v}_3 d^3 \mathbf{v}_4 \delta_{12 \rightarrow 34} W_{12 \rightarrow 34} \times [f(\mathbf{r}, \mathbf{v}_1) f(\mathbf{r}, \mathbf{v}_2) - f(\mathbf{r}, \mathbf{v}_3) f(\mathbf{r}, \mathbf{v}_4)], \quad (8.5)$$

where  $W_{12 \rightarrow 34} = W_{43 \rightarrow 12}$  are the collision rates. The factor  $1/4$  cancels the fact that each collision process ( $1 \leftrightarrow 3, 2 \leftrightarrow 4$ ) is counted four times.

Changing variables in the integral, using the center of mass velocity and the angle of deviation in the center of mass frame,  $W$  is

$$W_{12 \rightarrow 34} = |\mathbf{v}_2 - \mathbf{v}_1| \frac{\sigma}{4\pi}, \quad (8.6)$$

with  $\sigma = 8\pi/k^2$ , where  $k = |\mathbf{v}_2 - \mathbf{v}_1|/m/(2\hbar)$  is the wave vector of the relative motion.

Equation (8.5) alone does not give the evolution of the distribution  $f$ . In general, one has to solve the Boltzmann equation. But, in the collisionless regime, where the time between two collisions is much longer than the oscillation period of the atoms in the trap, the problem can be simplified. In this regime, we do not expect oscillations of the cloud and we can assume that, for both the vertical and horizontal motion, the distribution  $f$  corresponds to a Boltzmann distribution with temperatures  $T_z$  and  $T_p$  which may be different.

With such an ansatz for  $f$ , and noting that

$$\Delta E = NK_D(T_z - T_p), \quad (8.7)$$

Eq. (8.5) gives a differential equation for  $T_z - T_p$ . For small initial deviations from equilibrium, we can linearize the equation in  $T_z - T_p$ . With this approximation, the evolution is exponential with a  $1/e$  time constant

$$T_{\text{therm}} = \frac{15\sqrt{\pi}}{2} \frac{1}{\bar{n} \frac{8\pi\hbar^2}{\left(\frac{m}{2}\right)^2 k_B T_0} \left(\frac{k_B T_0}{m}\right)^{1/2}}, \quad (8.8)$$

where  $T_0$  is the equilibrium temperature and  $\bar{n}$  is the mean density.

We thus find that

$$\frac{1}{\bar{n} v_{\text{rms}} T_{\text{therm}}} = \frac{2}{15\sqrt{\pi}} \sigma(v_{\text{rms}}) = \frac{64\sqrt{\pi}}{15} \frac{\hbar^2}{m k_B T_0}, \quad (8.9)$$

where  $\sigma(v_{\text{rms}})$  is the cross section for a relative velocity  $v_{\text{rms}} = \sqrt{k_B T_0}/m$ .

As expected, the quantity  $1/\bar{n} v_{\text{rms}} T_{\text{therm}}$  is inversely proportional to the temperature. We have thus obtained the numerical factors entering in Eq. (8.9), which are plotted in Fig. 10.

### E. Inhibition of thermalization when $k_B T \ll \hbar \omega_{\text{osc}}$

We now give a simple physical interpretation of the exponential decrease of the thermalization rate between the horizontal and vertical degrees of freedom previously found in Ref. [21]. We show that this behavior is due to the quantization of the energy levels in the vertical direction and to parity conservation during the collision process.

The collision rate is

$$\Gamma_{\text{coll}} \approx n v \sigma, \quad (8.10)$$

where  $n$  is the three-dimensional density,  $v$  is the typical velocity of the atoms, and  $\sigma$  is the typical cross section. For  $k_B T \ll \hbar \omega_{\text{osc}}$ , the horizontal velocity of the atoms is much smaller than the typical vertical velocity  $\sqrt{\hbar \omega_{\text{osc}}}/(2m)$  and

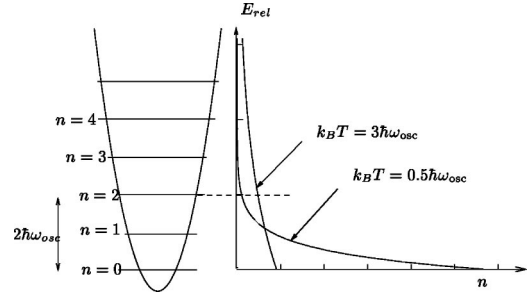


FIG. 11. Probability distribution of the relative kinetic energy of the horizontal motion of a pair of atoms for a temperature of  $3\hbar\omega_{\text{osc}}/k_B$  (initial conditions in our experiments) and a temperature of  $0.5\hbar\omega_{\text{osc}}/k_B$  (end of 1D sideband cooling).

the 3D density is  $n = n_{2D} \sqrt{2m/(\omega_{\text{osc}}\hbar)}$ , where  $n_{2D}$  is the 2D density. Thus the collisional rate satisfies

$$\Gamma_{\text{coll}} \approx \frac{\hbar n_{2D}}{m}. \quad (8.11)$$

$\Gamma_{\text{coll}}^{-1}$  is an estimate of the thermalization time between the two horizontal degrees of freedom, in agreement with the rigorous calculation of Ref. [21] as long as the temperature is not extremely small [32].

On the other hand, the thermalization between the horizontal and the vertical degrees of freedom actually takes a much longer time. Indeed, the energy levels are quantized in the vertical direction. In order to transfer energy to the vertical motion during a collision, the horizontal kinetic energy of the atoms has to be at least  $\hbar\omega_{\text{osc}}$  before the collision. In fact, because of parity conservation, only the vibrational state  $|n=2\rangle$  of the relative motion can be populated after the collision [21]. Thus, the horizontal energy of the pair of colliding atoms has to be at least  $2\hbar\omega_{\text{osc}}$ . Figure 11 presents the probability distribution  $n(E)$  of the kinetic energy of the relative horizontal motion of a pair of atoms, for a temperature of  $3\hbar\omega_{\text{osc}}$  and a temperature of  $0.5\hbar\omega_{\text{osc}}$  close to the value achieved in our experiments. Because the density of states is constant in two dimensions, at a temperature  $T$ ,  $n(E) = 1/(k_B T) \exp(-E/(k_B T))$ . Thus, the probability that a colliding pair has an energy large enough to populate the excited states of the vertical motion is

$$p = \exp(-2\hbar\omega_{\text{osc}}/k_B T). \quad (8.12)$$

Among the collisions transferring energy to the vertical motion, we can neglect the exponentially small amount that will transfer an energy larger than  $2\hbar\omega_{\text{osc}}$ . Thus, the rate of change of the vertical energy is

$$\frac{dE_z}{dt} \approx 2\hbar\omega_{\text{osc}} \frac{\hbar n_{2D}}{m} \exp(-2\hbar\omega_{\text{osc}}/k_B T). \quad (8.13)$$

This exponential factor is responsible for the drastic inhibition of the cooling of the horizontal motion near  $k_B T \approx \hbar\omega_{\text{osc}}$  as already discussed in Sec. V.

On the other hand, the increase of the vertical energy needed to reach the thermal equilibrium is, neglecting the change of horizontal temperature,

$$\Delta E_z = \hbar \omega_{\text{osc}} \exp(-\hbar \omega_{\text{osc}}/k_B T). \quad (8.14)$$

Thus, the thermalization time  $T_{\text{therm}}$  is of the order of

$$\frac{1}{T_{\text{therm}}} \approx \frac{1}{\Delta E_z} \frac{dE_z}{dt} \sim \frac{n_{2D} \hbar}{m} \exp(-\hbar \omega_{\text{osc}}/k_B T). \quad (8.15)$$

This formula is identical, within a numerical factor, to the formula of Ref. [21] using a quantum treatment of collisions in 2D. It is interesting to note that both  $dE_z/dt$  and  $\Delta E_z$  are exponentially small but it is the difference in the exponents that explains the exponential factor of  $T_{\text{therm}}$ .

The most efficient way to detect this exponential dependence of  $T_{\text{therm}}$  would be to compare the thermalization time between the two horizontal degrees of freedom ( $\approx \hbar n_{2D}/m$ ) to the thermalization time between them and the vertical motion. However when the initial horizontal temperature is  $k_B T \ll \hbar \omega_{\text{osc}}$ , even if the initial vertical temperature is  $\approx 0$ , the relaxation towards equilibrium corresponds to an exponentially small change of the horizontal temperature and an exponentially small population in the excited vibrational states. The observation of these small changes would require a very sensitive measurement of the temperature or of the population of the vertical vibrational states. Therefore, the easiest choice of parameters to detect this 2D behavior is to operate near  $k_B T \approx \hbar \omega_{\text{osc}}$ .

## IX. SUMMARY

In this paper, we have investigated 1D sideband cooling of cesium atoms in a far-detuned optical lattice. This cooling

is particularly efficient because, for each spontaneously emitted photon, an energy of order  $\hbar \omega_{\text{osc}}$  is removed from the system. Atoms are spin polarized in  $F=3$  and, at high density, elastic collisions enable 3D cooling of the sample through 1D sideband cooling. We have produced atomic samples in which more than 80% of the atoms are in the vibrational ground state of motion in 1D and with a transverse temperature of  $0.7 \hbar \omega_{\text{osc}}/k_B = 2.8 \mu\text{K}$ . This realizes a quasi-2D cold gas. Limitations of this cooling method have been identified. First, light-induced atom losses have been observed. Second, cooling of the weakly confined degrees of freedom by collisions loses its efficiency around  $k_B T \approx \hbar \omega_{\text{osc}}$ . We explained this effect by an exponential slowing down of the energy transfer between the weakly and strongly confined degrees of freedom. A dynamic method involving changes of the high oscillation frequency via polarization rotation of one of the trapping beams has been proposed and implemented. We have shown that the zero energy scattering resonance of cesium was essentially unaffected in the temperature range 4–20  $\mu\text{K}$ . Within our experimental accuracy, this is in agreement with theoretical calculations. Further studies could concentrate on collisions affecting only the motion in the weak confinement directions where dramatic modifications of collisions occur at  $k_B T \approx 0.1 \hbar \omega_{\text{osc}}$  [4,21]. Promising systems for these studies are Bose-Einstein condensates loaded in a far-detuned trap associated with the possibility of manipulating the scattering length via Feshbach resonances.

## ACKNOWLEDGMENTS

We gratefully thank Gora Shlyapnikov for help in theory and interesting discussions. Laboratoire Kastler Brossel is unité de recherche de l'Ecole Normale Supérieure et de l'Université Pierre et Marie Curie, associée au CNRS. M. Morinaga thanks the University of Tokyo for its support.

- 
- [1] A. I. Safonov *et al.*, Phys. Rev. Lett. **81**, 4545 (1998).
  - [2] J. Walraven, in *Fundamental Systems in Quantum Optics*, Proceedings of the Les Houches Summer School, Session LIII, edited by J. R. J. Dalibard and J. Zinn-Justin (Elsevier Science, Amsterdam, 1992).
  - [3] See *Bose-Einstein Condensation in Atomic Gases*, Proceedings of the International School of Physics ‘‘Enrico Fermi,’’ edited by M. Inguscio *et al.* (IOS, Amsterdam, 1998).
  - [4] D. S. Petrov, M. Holzmann, and G. V. Shlyapnikov, Phys. Rev. Lett. **84**, 2551 (2000).
  - [5] D. S. Petrov, G. V. Shlyapnikov, and J. T. M. Walraven, Phys. Rev. Lett. **85**, 3745 (2000).
  - [6] P. Leo, C. Williams, and P. Julienne, Phys. Rev. Lett. **85**, 2721 (2000).
  - [7] P. Ruprecht, M. Holland, K. Burnett, and M. Edwards, Phys. Rev. A **51**, 4704 (1995).
  - [8] V. Vuletić, C. Chin, A. Kerman, and S. Chu, Phys. Rev. Lett. **81**, 5768 (1998).
  - [9] S. E. Hammann *et al.*, Phys. Rev. Lett. **80**, 4149 (1998).
  - [10] H. Perrin, A. Kuhn, I. Bouchoule, and C. Salomon, Europhys. Lett. **42**, 395 (1998).
  - [11] I. Bouchoule *et al.*, Phys. Rev. A **59**, R8 (1999).
  - [12] F. Diedrich, J. C. Berquist, W. M. Itano, and D. J. Wineland, Phys. Rev. Lett. **62**, 403 (1989).
  - [13] D.-J. Han *et al.*, Phys. Rev. Lett. **85**, 724 (2000).
  - [14] R. Grimm, Adv. At., Mol. Opt. Phys. **42**, 95 (2000).
  - [15] H. Gauck *et al.*, Phys. Rev. Lett. **81**, 5298 (1998).
  - [16] M. Hammes *et al.*, J. Mod. Opt. **47**, 2755 (2000).
  - [17] R. Scheunemann, F. S. Cataliotti, T. W. Hänsch, and M. Weitz, Phys. Rev. A **62**, 051801 (2000).
  - [18] M. Arndt *et al.*, Phys. Rev. Lett. **79**, 625 (1997).
  - [19] D. Guéry-Odelin, J. Söding, P. Desbiolles, and J. Dalibard, Opt. Express **2**, 323 (1998).
  - [20] S. A. Hopkins *et al.*, Phys. Rev. A **61**, 032707 (2000).
  - [21] D. S. Petrov and G. V. Shlyapnikov, Phys. Rev. A **64**, 012706 (2001).
  - [22] M. Morinaga, I. Bouchoule, J. C. Karam, and C. Salomon, Phys. Rev. Lett. **83**, 4037 (1999).
  - [23] V. Vuletić, A. Kerman, C. Chin, and S. Chu, Phys. Rev. Lett. **82**, 1406 (1999).
  - [24] H. Perrin *et al.*, Europhys. Lett. **46**, 141 (1999).

- [25] D. J. Wineland and W. M. Itano, *Phys. Rev. A* **20**, 1521 (1979).
- [26] J. Javanainen, *J. Opt. Soc. Am. B* **1**, 111 (1984).
- [27] M. Lindberg, *J. Phys. B* **17**, 2129 (1984).
- [28] P. S. Julienne, in *Laser Manipulation of Atoms and Ions*, Proceedings of the International School of Physics "Enrico Fermi" (North-Holland, Amsterdam, 1992), p. 746.
- [29] A. Gallagher and D. E. Pritchard, *Phys. Rev. Lett.* **63**, 957 (1989).
- [30] P. S. Julienne and J. Vigué, *Phys. Rev. A* **44**, 4464 (1991).
- [31] L. Landau and E. Lifchitz, *Mechanics* (Pergamon, Oxford, 1978).
- [32] A logarithmic decrease of the collision rate with the inverse of the temperature is expected when  $k_B T \ll 0.05 \hbar \omega_{\text{osc}}$  [4].